First observation of the decay $B\_s^0 \to K^-\mu^+\nu\_\mu$ and Measurement of $|V\_ub|/|V\_cb|$

R. Aaij, C. Abellán Beteta, T. Ackernley, B. Adeva, M. Adinolfi, H. Afsharnia, C.A. Aidala, S. Aiola, Z. Ajaltouni, S. Akar, et al.

First Observation of the Decay $B_s^0 \to K^-\mu^+\nu_\mu$ and a Measurement of $|V_{ub}|/|V_{cb}|$

R. Aaij *et al.*[*]
(LHCb Collaboration)

(Received 9 December 2020; accepted 21 January 2021; published 25 February 2021)

The first observation of the suppressed semileptonic $B_s^0 \to K^-\mu^+\nu_\mu$ decay is reported. Using a data sample recorded in pp collisions in 2012 with the LHCb detector, corresponding to an integrated luminosity of 2 fb^{-1}, the branching fraction $\mathcal{B}(B_s^0 \to K^-\mu^+\nu_\mu)$ is measured to be $[1.06 \pm 0.05(\text{stat}) \pm 0.08(\text{syst})] \times 10^{-4}$, where the first uncertainty is statistical and the second one represents the combined systematic uncertainties. The decay $B_s^0 \to D_s^-\mu^+\nu_\mu$, where D_s^- is reconstructed in the final state $K^+K^-\pi^-$, is used as a normalization channel to minimize the experimental systematic uncertainty. Theoretical calculations on the form factors of the $B_s^0 \to K^-$ and $B_s^0 \to D_s^-$ transitions are employed to determine the ratio of the Cabibbo-Kobayashi-Maskawa matrix elements $|V_{ub}|/|V_{cb}|$ at low and high $B_s^0 \to K^-$ momentum transfer.

DOI: 10.1103/PhysRevLett.126.081804

The coupling of the electroweak interaction between up- and down-type quarks is modulated by the Cabibbo-Kobayashi-Maskawa (CKM) matrix [1,2]. Hadrons containing a b quark can decay weakly via a virtual W boson to semileptonic final states through the tree-level transitions $b \to c(W^* \to \ell\nu)$ and $b \to u(W^* \to \ell\nu)$, where $\ell\nu$ denotes a charged lepton and a neutrino. These transitions involve the CKM matrix elements V_{cb} and V_{ub}, respectively, which obey the observed hierarchy $|V_{ub}|/|V_{cb}| \sim 0.1$, resulting in the transitions $b \to c\ell\nu$ being favored over $b \to u\ell\nu$. Semileptonic b hadron decays are an excellent ground for measuring $|V_{cb}|$ and $|V_{ub}|$ since the factorization of the hadronic and leptonic parts of the amplitudes eases theoretical calculations [3,4]. Improving the precision on the measurements of the CKM elements can be exploited to probe possible deviations from the standard model of particle physics [5]. Existing $|V_{ub}|$ and $|V_{cb}|$ measurements show a discrepancy between those performed with exclusive decays, where all the visible particles are reconstructed, and inclusive decays where only the lepton is reconstructed [6]. The world average of the exclusive $|V_{ub}|$ results is dominated by $B^0 \to \pi^-\ell^+\nu_\ell$ measurements. The LHCb measurement using the baryonic decays $\Lambda_b^0 \to p\mu^-\bar{\nu}_\mu$ and $\Lambda_b^0 \to \Lambda_c^+\mu^-\bar{\nu}_\mu$ [7] gives the ratio $|V_{ub}|/|V_{cb}| = 0.079 \pm 0.006$, as updated in Ref. [6]. In addition to the inclusive versus exclusive puzzle, measurements of $|V_{ub}|/|V_{cb}|$ are important to constrain the CKM unitarity triangle [8,9].

This Letter reports the first observation of the decay $B_s^0 \to K^-\mu^+\nu_\mu$, the measurement of its branching fraction and of the ratio $|V_{ub}|/|V_{cb}|$ with $B_s^0 \to D_s^-\mu^+\nu_\mu$ as a normalization channel [10]. The measurement of the branching fraction is performed in two regions of the $B_s^0 \to K^-$ momentum transfer or invariant mass squared of the muon and the neutrino q^2, as well as integrated over the full q^2 range. The ratio $|V_{ub}|/|V_{cb}|$ is derived in the two q^2 regions using calculations of the form factors of the $B_s^0 \to K^-$ and $B_s^0 \to D_s^-$ transitions based on both light cone sum rule (LCSR) [11,12] and lattice QCD (LQCD) [13] methods. The data sample consists of pp collisions recorded by the LHCb detector in 2012 at a center-of-mass energy of 8 TeV corresponding to 2 fb^{-1} of integrated luminosity. The LHCb detector is a single-arm forward spectrometer covering the pseudorapidity range $2 < \eta < 5$, described in detail in Refs. [14,15]. The trigger [16] consists of a hardware stage, based on information from the calorimeter and muon systems, followed by a software stage, which reconstructs charged particles. Simulation, produced with software packages described in Refs. [17–19], is used to model the effects of the detector acceptance and the imposed selection requirements.

In this analysis, candidates for $B_s^0 \to K^-\mu^+\nu_\mu$ and $B_s^0 \to D_s^-\mu^+\nu_\mu$ decays are formed by combining a muon with a kaon or a D_s^- candidate reconstructed through the decay $D_s^- \to K^+K^-\pi^-$. The trigger and initial selection requirements are chosen to be similar between these two modes. Events are retained by the hardware trigger due to the presence of a high-p_T muon, where p_T is the momentum component transverse to the beam. The software trigger [20] selects partially reconstructed B decays by combining

[*]Full author list given at the end of the article.

a track or a D_s^- candidate with a well identified muon candidate. The initial selection includes requirements on the track kinematics and quality, particle identification, as well as on the B_s^0 candidate kinematics and decay topology. The obtained samples for each of the decays include background contributions dominated by b hadron decays with additional tracks or neutral particles in the final state. For the $K^-\mu^+$ combinations, the main background originates from $H_b \to \mu^+ H_c(\to K^- X)X'$, where $H_{b,c}$ represents a hadron containing a b or a c quark and $X^{(\prime)}$ denotes unreconstructed particles. Decays to excited K^* resonances, $B_s^0 \to K^{*-}(\to K^-\pi^0)\mu^+\nu_\mu$, and charmonium modes $B \to [c\bar{c}](\to \mu^+\mu^-)K^- X$, where $[c\bar{c}] = J/\psi, \psi(2S)$, are secondary background contributions. Other sources arise from b hadron decays where a track is misidentified as a kaon or a muon and random combinations of a muon and a kaon. In the $D_s^-\mu^+$ combinations, the main (and irreducible) source of background arises from $B_s^0 \to D_s^{*-}(\to D_s^-\gamma)\mu^+\nu_\mu$ decays. Additional contributions include decays to higher excitations of the D_s^- meson, $B_s^0 \to D_s^{**-}(\to D_s^- X)\mu^+\nu_\mu$, double-charm decays of the type $B_{u,d,s} \to D_s DX$ and semitauonic $B_s^0 \to D_s^-\tau^+\nu_\tau$ decays.

To suppress background, the $K^-\mu^+$ and $D_s^-\mu^+$ candidates are required to be isolated from other tracks in the event. A multivariate algorithm (MVA) is trained to determine if a given track originates from the candidate or from the rest of the event (ROE). A threshold on the value of the MVA output is applied to the ROE track that appears to be the closest to the signal. For $K^-\mu^+$ candidates, two boosted decision tree (BDT) classifiers [21,22] are used sequentially to further reduce the remaining background. A *charged* BDT classifier is trained against a mixture of the main background components using, in addition to the isolation MVA output, invariant masses formed by the least isolated ROE track with respect to each of the muon or the kaon, and variables related to the B_s^0, K^-, and μ^+ kinematics. The background passing the charged BDT requirement comprises decays without an additional track, mainly of the type $H_b \to \mu^+ H_c(\to K^- P)$, where P is either a long-lived or a neutral particle. A second BDT classifier, denoted *neutral* BDT, involves kinematic variables of the K^- and B_s^0 candidates, the B_s^0 vertex position and quality, the invariant mass formed by the signal kaon, and any π^0 meson in its vicinity; it also exploits the asymmetry between the kaon momentum and an average momentum direction formed by neutral particles in the vicinity of the kaon. The shapes of the BDT outputs are calibrated with the decay $B^- \to J/\psi(\to \mu^+\mu^-)K^-$, which is reconstructed both as a $K^-\mu^+$ candidate and fully reconstructed where the least isolated track near the $K^-\mu^+$ pair is identified as μ^-. Kinematic weighting accounts for data-simulation discrepancies for the training of the classifiers.

The B_s^0 mass is represented by the corrected mass [23], defined as

$$m_{\rm corr} = \sqrt{m_{Y\mu}^2 + p_\perp^2/c^2} + p_\perp/c, \tag{1}$$

where $m_{Y\mu}$ is the invariant mass of the $Y\mu$ pair, with $Y = K^-$ or D_s^-, and $p_\perp$ is the momentum of this pair transverse to the B_s^0 flight direction. The flight direction is defined as the vector between the positions of the primary pp collision vertex and the B_s^0 decay vertex. In order to improve the separation between the $B_s^0 \to K^-\mu^+\nu_\mu$ signal and background, the uncertainty on $m_{\rm corr}$ is required to be $\sigma(m_{\rm corr}) < 100\ {\rm MeV}/c^2$. The shape of $\sigma(m_{\rm corr})$ is calibrated following a similar procedure as for the BDT classifiers. To derive q^2, the neutrino momentum is estimated using the B_s^0 flight direction and the known B_s^0 mass. A twofold ambiguity resulting from this estimate is resolved by choosing the solution that is most consistent with the B_s^0 momentum predicted by a linear regression method [24]. The fit to the $m_{\rm corr}$ distribution, used for the extraction of the $B_s^0 \to K^-\mu^+\nu_\mu$ signal, is performed in two q^2 regions, respectively, above and below $7\ {\rm GeV}^2/c^4$ ("high" and "low"), which are chosen to contain approximately the same expected signal yields.

For the $B_s^0 \to D_s^-\mu^+\nu_\mu$ decay, a fit to the invariant mass of the $D_s^- \to K^+K^-\pi^-$ candidates is performed in 40 intervals of $m_{\rm corr}$ from 3000 to 6500 ${\rm MeV}/c^2$. his provides the D_s yield as a function of $m_{\rm corr}$ and thus subtracts the background originating from combinations of random kaon and pion tracks. The obtained $m_{\rm corr}$ distribution is fit to extract the $B_s^0 \to D_s^-\mu^+\nu_\mu$ signal yield. For the $B_s^0 \to K^-\mu^+\nu_\mu$ decay, the combinatorial background is largely reduced by applying a topological criterion: the opening angle between the directions of the K^- and μ^+ candidates in the plane transverse to the pp collision axis is required to be less than 90°. The efficiency of this requirement on the signal is 93%, while it removes approximately 90% of the combinatorial background.

The efficiencies of the signal and normalization channels are derived from simulation and take into account the effects of the triggers, reconstruction, selection, particle identification, isolation procedure, MVA requirements, and detector acceptance. Data-driven corrections are applied to account for any mismodeling related to the kinematics, number of tracks in the event, and particle identification variables. The efficiency ratio between the signal and normalization decays is $\epsilon_K/\epsilon_{D_s} = 1.109 \pm 0.018$, 0.553 ± 0.009, and 0.733 ± 0.009 for $q^2 < 7\ {\rm GeV}^2/c^4$, $q^2 > 7\ {\rm GeV}^2/c^4$, and the full q^2 range, respectively. The uncertainties reflect the limited size of the simulated samples.

The fit template for the $m_{\rm corr}$ distribution of the $B_s^0 \to K^-\mu^+\nu_\mu$ signal is obtained from simulation, while the shapes for the background components are derived from either simulation or control samples. The statistical uncertainties originating from the finite samples used to obtain

the templates are accounted for in the fits [25]. The main background $H_b \to H_c(\to K^- X)\mu^+ X'$, whose yield is free in the fit, is obtained with a simulated inclusive sample. The $B_s^0 \to K^{*-}(\to K^-\pi^0)\mu^+\nu_\mu$ background is modeled by simulating a mixture of three resonances [$K^{*-}(892)$, $K_0^{*-}(1430)$, and $K_2^{*-}(1430)$] with a substantial branching fraction to the $K^-\pi^0$ final state. Though the overall yield is free, the mixture is fixed to certain proportions that are varied up to a factor of 2.5 for systematic studies, according to available measurements of the decays $B^- \to K^{*-}\mu^+\mu^-$ and $B^- \to K^{*-}\eta/\phi$ [26]. The impact of a possible $B_s^0 \to K^-\pi^0\mu^+\nu_\mu$ nonresonant decay has also been considered and found to be absorbed by the resonant mixture. The charmonium background is dominated by $B^- \to J/\psi(\to \mu^+\mu^-)K^- X$ decays, with the fraction of the $B^- \to J/\psi(\to \mu^+\mu^-)K^-$ channel exceeding 75%. Its shape is determined with simulated $B^- \to J/\psi(\to \mu^+\mu^-)K^- X$ events, while its yield is derived from the yield of the $B^- \to J/\psi(\to \mu^+\mu^-)K^-$ signal peak in data. To recover that peak from $K^-\mu^+$ combinations, the missing momentum of the μ^- is calculated from the B^- flight direction and the known J/ψ mass. The background originating from the misidentification (misID) of a pion, proton, or muon as a kaon—or a kaon, proton, or pion as a muon—is modeled using data samples of $h\mu^+$ ($K^- h$) candidates with an identical selection as for the main sample, but where h is a charged track that fails the kaon (muon) identification criteria. These control samples are thus enriched in misidentified tracks of the different species. The different contributions to the kaon and muon misID are unfolded using control samples of kinematically identified hadrons and muons [27]. These samples are used to derive the probabilities that a particle belonging to a given species and with particular kinematic properties would pass the kaon or muon criteria. With this method, both the $m_{\rm corr}$ shape and the yield of the misID are constrained. The combinatorial background is modeled with a separate data sample, where a kaon and a muon from different events are combined. The obtained pseudocandidates undergo the same selection as the signal candidates and are corrected to reproduce the kinematic properties of the standard candidates. The fit to the normalization channel $B_s^0 \to D_s^-\mu^+\nu_\mu$ employs shapes obtained from simulation. The $B_s^0 \to D_s^-\mu^+\nu_\mu$ decay is modeled with the recent form factor predictions of Ref. [28]. The main background originates from B_s^0 semimuonic decays to excitations of the D_s^- meson, with the dominant $D_s^{*-} \to D_s^-\gamma$ decay represented by a specific shape, and higher excitations $D_s^{**-} = [D_{s0}^{*-}(2317), D_{s1}^-(2460), D_{s1}^-(2536)] \to D_s^- X$ modeled by a combined shape. Other sources of background are the decays of the form $B \to D_s^- DX$ and the semitauonic decay $B_s^0 \to D_s^-\tau^+(\to \mu^+\nu_\mu\bar{\nu}_\tau)\nu_\tau$. Because of the similarity of

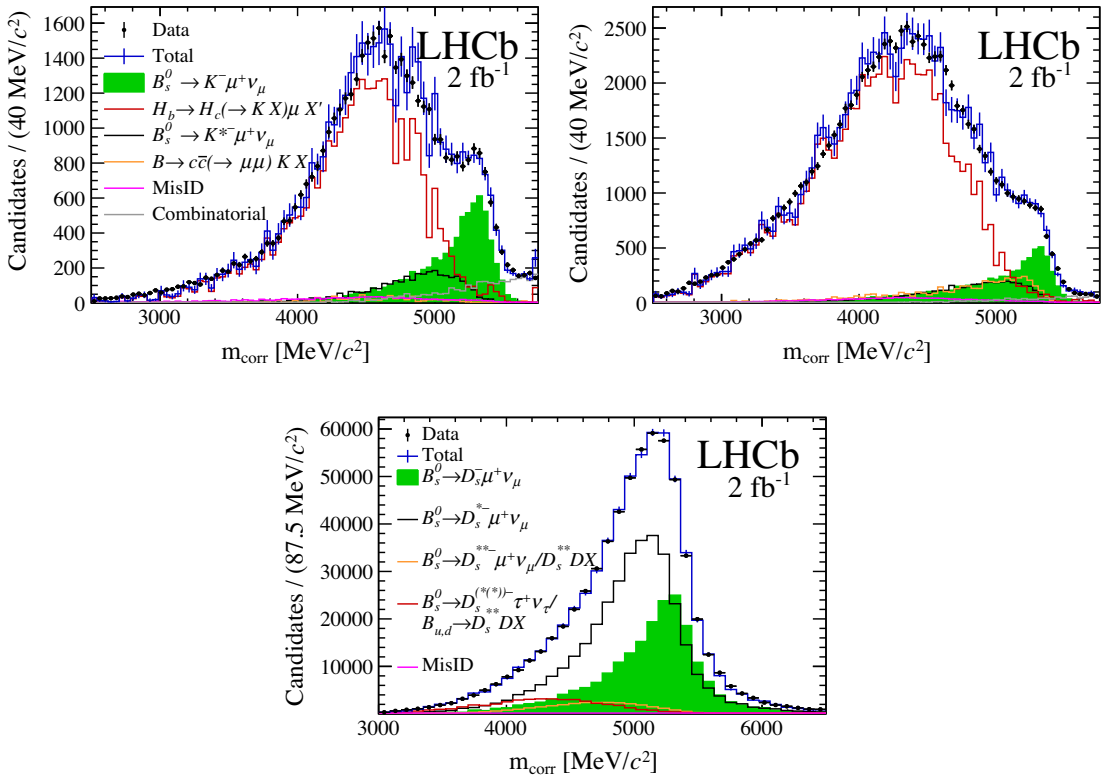

FIG. 1. Distribution of $m_{\rm corr}$ for (top) the signal $B_s^0 \to K^-\mu^+\nu_\mu$, with (left) $q^2 < 7$ GeV$^2/c^4$ and (right) $q^2 > 7$ GeV$^2/c^4$, and (bottom) the normalization $B_s^0 \to D_s^-\mu^+\nu_\mu$ channel. The points represent data, while the resulting fit components are shown as histograms.

their shapes, the $B_s^0 \to D_s^{**-}\mu^+\nu_\mu$ channels are grouped with $B_s \to D_s^- DX$ decays, while $B_s^0 \to D_s^-\tau^+(\to \mu^+\nu_\mu\bar{\nu}_\tau)\nu_\tau$ is combined with $B_{u,d} \to D_s^- DX$ decays.

The corrected mass distributions of the signal and normalization candidates are shown in Fig. 1, with the binned maximum-likelihood fit projections overlaid. The $B_s^0 \to K^-\mu^+\nu_\mu$ yields for $q^2 < 7$ and $q^2 > 7\ \mathrm{GeV}^2/c^4$ regions are found to be $N_K = 6922 \pm 285$ and 6399 ± 370, respectively, while the $B_s^0 \to D_s^-\mu^+\nu_\mu$ yield is $N_{D_s} = 201450 \pm 5200$. The uncertainties include both the effect of the limited dataset and the finite size of the samples used to derive the fit templates. Unfolding the two effects in quadrature shows that they have similar sizes.

This is the first observation of the decay $B_s^0 \to K^-\mu^+\nu_\mu$. The ratio of branching fractions is inferred as

$$R_{\mathrm{BF}} \equiv \frac{\mathcal{B}(B_s^0 \to K^-\mu^+\nu_\mu)}{\mathcal{B}(B_s^0 \to D_s^-\mu^+\nu_\mu)} = \frac{N_K}{N_{D_s}}\frac{\epsilon_{D_s}}{\epsilon_K} \times \mathcal{B}(D_s^- \to K^+K^-\pi^-), \tag{2}$$

with $\mathcal{B}(D_s^- \to K^+K^-\pi^-) = (5.39 \pm 0.15)\%$ [26] and gives

$$\begin{aligned} R_{\mathrm{BF}}(\mathrm{low}) &= [1.66 \pm 0.08(\mathrm{stat}) \pm 0.07(\mathrm{syst}) \\ &\quad \pm 0.05(D_s)] \times 10^{-3}, \\ R_{\mathrm{BF}}(\mathrm{high}) &= [3.25 \pm 0.21(\mathrm{stat})^{+0.16}_{-0.17}(\mathrm{syst}) \\ &\quad \pm 0.09(D_s)] \times 10^{-3}, \\ R_{\mathrm{BF}}(\mathrm{all}) &= [4.89 \pm 0.21(\mathrm{stat})^{+0.20}_{-0.21}(\mathrm{syst}) \\ &\quad \pm 0.14(D_s)] \times 10^{-3}, \end{aligned}$$

where the uncertainties are statistical, systematic, and due to the $D_s^- \to K^+K^-\pi^-$ branching fraction. Table I summarizes the systematic uncertainties. It includes uncertainties on the calibration and correction of the track reconstruction, trigger, particle identification, selection variables, migration of events between q^2 regions, efficiencies, and the fit template distributions. The largest systematic uncertainty originates from the fit templates and is evaluated by varying the shape of the fit components according to alternative models and also by modifying within its uncertainty the mixture of exclusive decays representing some of the background contributions. In particular, the signal shape is varied using various form factor models [29–32]. A similar procedure is applied to the normalization channel. The tracking uncertainty comprises the limited precision on tracking efficiency corrections obtained from control samples in data and the uncertainty on modeling the hadronic interactions with the detector material. The uncertainty on the q^2 migration is related to the limited accuracy of the evaluation of the cross feed between low- and high-q^2 regions in simulation.

TABLE I. Relative systematic uncertainties on the ratio $\mathcal{B}(B_s^0 \to K^-\mu^+\nu_\mu)/\mathcal{B}(B_s^0 \to D_s^-\mu^+\nu_\mu)$, in percent.

Uncertainty	All q^2	Low q^2	High q^2
Tracking	2.0	2.0	2.0
Trigger	1.4	1.2	1.6
Particle identification	1.0	1.0	1.0
$\sigma(m_{\mathrm{corr}})$	0.5	0.5	0.5
Isolation	0.2	0.2	0.2
Charged BDT	0.6	0.6	0.6
Neutral BDT	1.1	1.1	1.1
q^2 migration	⋯	2.0	2.0
Efficiency	1.2	1.6	1.6
Fit template	$^{+2.3}_{-2.9}$	$^{+1.8}_{-2.4}$	$^{+3.0}_{-3.4}$
Total	$^{+4.0}_{-4.3}$	$^{+4.3}_{-4.5}$	$^{+5.0}_{-5.3}$

To determine the branching fraction $\mathcal{B}(B_s^0 \to K^-\mu^+\nu_\mu)$ and the ratio $|V_{ub}|/|V_{cb}|$, the predicted integrals of the form factors $\mathrm{FF}_Y = |V_{xb}|^{-2}\int[d\Gamma(B_s^0 \to Y\mu^+\nu_\mu)/dq^2]dq^2$ ($Y = K^-,\ D_s^-;\ x = u,\ c$) are required. The absolute branching fraction is calculated as $\mathcal{B}(B_s^0 \to K^-\mu^+\nu_\mu) = \tau_{B_s} \times |V_{cb}|^2 \times \mathrm{FF}_{D_s} \times R_{\mathrm{BF}}$. The inputs are the exclusive value of $|V_{cb}| = (39.5 \pm 0.9) \times 10^{-3}$ [26], the B_s^0 meson lifetime $\tau_{B_s} = 1.515 \pm 0.004$ ps [26], and the form factor integral $\mathrm{FF}_{D_s} = 9.15 \pm 0.37\ \mathrm{ps}^{-1}$ based on a recent LQCD computation [28]. This leads to

$$\begin{aligned} \mathcal{B}(B_s^0 \to K^-\mu^+\nu_\mu) &= [1.06 \pm 0.05(\mathrm{stat}) \pm 0.04(\mathrm{syst}) \\ &\quad \pm 0.06(\mathrm{ext}) \pm 0.04(\mathrm{FF})] \times 10^{-4}, \end{aligned}$$

where the uncertainties are statistical, systematic, from the external inputs (D_s^- branching fraction, B_s^0 lifetime, and $|V_{cb}|$), and the $B_s^0 \to D_s^-$ form factor integral, respectively. Combining the systematic uncertainties, the branching fraction is $\mathcal{B}(B_s^0 \to K^-\mu^+\nu_\mu) = [1.06 \pm 0.05(\mathrm{stat}) \pm 0.08(\mathrm{syst})] \times 10^{-4}$.

The ratio of CKM elements $|V_{ub}|/|V_{cb}|$ is obtained through the relation $R_{\mathrm{BF}} = |V_{ub}|^2/|V_{cb}|^2 \times \mathrm{FF}_K/\mathrm{FF}_{D_s}$. For the FF_K value, a recent LQCD prediction is used for the high-q^2 range, $\mathrm{FF}_K(q^2 > 7\ \mathrm{GeV}^2/c^4) = 3.32 \pm 0.46\ \mathrm{ps}^{-1}$ [31], while a LCSR calculation [32] is used for the low-q^2 range, $\mathrm{FF}_K(q^2 < 7\mathrm{GeV}^2/c^4) = 4.14 \pm 0.38\ \mathrm{ps}^{-1}$, due to the lower accuracy of LQCD calculations in this region. The obtained values are

$$\begin{aligned} |V_{ub}|/|V_{cb}|(\mathrm{low}) &= 0.0607 \pm 0.0015(\mathrm{stat}) \pm 0.0013(\mathrm{syst}) \\ &\quad \pm 0.0008\,(D_s) \pm 0.0030\,(\mathrm{FF}), \\ |V_{ub}|/|V_{cb}|(\mathrm{high}) &= 0.0946 \pm 0.0030(\mathrm{stat})^{+0.0024}_{-0.0025}(\mathrm{syst}) \\ &\quad \pm 0.0013\,(D_s) \pm 0.0068\,(\mathrm{FF}), \end{aligned}$$

where the latter two uncertainties are from the D_s^- branching fraction and the form factor integrals. The discrepancy between the values of $|V_{ub}|/|V_{cb}|$ for the low- and high-q^2

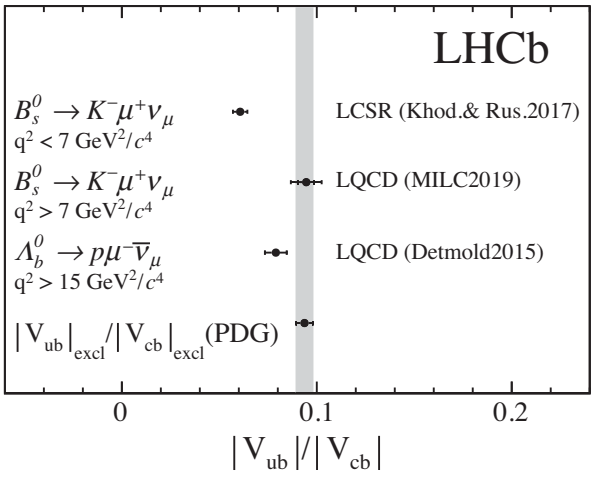

FIG. 2. Measurements of $|V_{ub}|/|V_{cb}|$ in this Letter and in Ref. [7] and ratio inferred from the Particle Data Group (PDG) [26] averages of exclusive $|V_{ub}|$ and $|V_{cb}|$ measurements, where the $\Lambda_b^0 \to p\mu^-\bar{\nu}_\mu$ result is not included. The form factor calculation used in each case is mentioned [31–33].

ranges is related to the difference in the theoretical calculations of the form factors. To illustrate this, the LQCD calculation in Ref. [31] gives $\mathrm{FF}_K = 0.94 \pm 0.48\ \mathrm{ps}^{-1}$ at low q^2, which can be compared to the chosen LCSR value, $4.14 \pm 0.38\ \mathrm{ps}^{-1}$ [32]. Figure 2 depicts the $|V_{ub}|/|V_{cb}|$ measurements of this Letter, $|V_{ub}|/|V_{cb}|(\mathrm{low}) = 0.061 \pm 0.004$ and $|V_{ub}|/|V_{cb}|(\mathrm{high}) = 0.095 \pm 0.008$, with the uncertainties combined. The $|V_{ub}|/|V_{cb}|$ measurement obtained with the Λ_b^0 baryon decays [7], for which a form factor model based on a LQCD calculation [33] was used, is also shown.

In conclusion, the decay $B_s^0 \to K^-\mu^+\nu_\mu$ is observed for the first time. The branching fraction ratios in the two q^2 regions reported in this Letter represent the first experimental ingredient to the form factor calculations of the $B_s^0 \to K^-\mu^+\nu_\mu$ decay. Moreover, the $|V_{ub}|/|V_{cb}|$ results will improve both the averages of the exclusive measurements in the $(|V_{cb}|, |V_{ub}|)$ plane and the precision on the least known side of the CKM unitarity triangle.

We express our gratitude to our colleagues in the CERN accelerator departments for the excellent performance of the LHC. We thank the technical and administrative staff at the LHCb institutes. We acknowledge support from CERN and from the national agencies CAPES, CNPq, FAPERJ, and FINEP (Brazil), MOST and NSFC (China), CNRS/IN2P3 (France), BMBF, DFG, and MPG (Germany), INFN (Italy), NWO (Netherlands), MNiSW and NCN (Poland), MEN/IFA (Romania), MSHE (Russia), MICINN (Spain), SNSF and SER (Switzerland), NASU (Ukraine), STFC (United Kingdom), and DOE NP and NSF (US). We acknowledge the computing resources that are provided by CERN, IN2P3 (France), KIT and DESY (Germany), INFN (Italy), SURF (Netherlands), PIC (Spain), GridPP (United Kingdom), RRCKI and Yandex LLC (Russia), CSCS (Switzerland), IFIN-HH (Romania), CBPF (Brazil), PL-GRID (Poland), and OSC (US). We are indebted to the communities behind the multiple open-source software packages on which we depend. Individual groups or members have received support from AvH Foundation (Germany), EPLANET, Marie Skłodowska-Curie Actions, and ERC (European Union), A*MIDEX, ANR, Labex P2IO, and OCEVU, and Région Auvergne-Rhône-Alpes (France), Key Research Program of Frontier Sciences of CAS, CAS PIFI, CAS CCEPP, Fundamental Research Funds for Central Universities, and Sci. and Tech. Program of Guangzhou (China), RFBR, RSF, and Yandex LLC (Russia), GVA, XuntaGal, and GENCAT (Spain), and the Royal Society and the Leverhulme Trust (United Kingdom).

[1] N. Cabibbo, Unitary symmetry and leptonic decays, Phys. Rev. Lett **10**, 531 (1963).
[2] M. Kobayashi and T. Maskawa, CP-Violation in the renormalizable theory of weak interaction, Prog. Theor. Phys **49**, 652 (1973).
[3] N. Isgur, D. Scora, B. Grinstein, and M. B. Wise, Semileptonic B and D decays in the quark model, Phys. Rev. D **39**, 799 (1989).
[4] M. J. Dugan and B. Grinstein, QCD basis for factorization in decays of heavy mesons, Phys. Lett. B **255**, 583 (1991).
[5] D. Abbaneo *et al.*, *Proceedings of the CKM Matrix and the Unitarity Triangle, CERN, Geneva, Switzerland, 2002* (CERN Yellow Reports, 2003), arXiv:hep-ph/0304132.
[6] Heavy Flavor Averaging Group, Y. Amhis *et al.*, Averages of b-hadron, c-hadron, and τ-lepton properties as of 2018, arXiv:1909.12524, updated results and plots available at https://hflav.web.cern.ch.
[7] R. Aaij *et al.* (LHCb Collaboration), Determination of the quark coupling strength $|V_{ub}|$ using baryonic decays, Nat. Phys. **11**, 743 (2015).
[8] CKMfitter Group, J. Charles, A. Höcker, H. Lacker, S. Laplace, F. R. Le Diberder, J. Malclés, J. Ocariz, M. Pivk, and L. Roos, CP violation and the CKM matrix: Assessing the impact of the asymmetric B factories, Eur. Phys. J. C **41**, 1 (2005), updated results and plots available at http://ckmfitter.in2p3.fr.
[9] M. Bona *et al.* (UTfit Collaboration), The unitarity triangle fit in the standard model and hadronic parameters from lattice QCD: A reappraisal after the measurements of Δm_s and $\mathrm{BR}(B \to \tau\nu)$, J. High Energy Phys. 10 (2006) 081, updated results and plots available at http://www.utfit.org/UTfit.
[10] Throughout the Letter, charge conjugate decays are implied.
[11] P. Colangelo and A. Khodjamirian, QCD sum rules, a modern perspective, at the frontier of particle physics 1495–1576, World Scientific, Report No. CERN-TH-2000-296, BARI-TH-2000-394, 2000.
[12] C. A. Dominguez, Introduction to QCD sum rules, Mod. Phys. Lett. A **28**, 1360002 (2013).

[13] H. J. Rothe, *Lattice Gauge Theories: An Introduction*, 4th ed., World Scientific Lecture Notes in Physics (World Scientific, Singapore, 2012), https://doi.org/10.1142/1268.
[14] A. A. Alves, Jr. *et al.* (LHCb Collaboration), The LHCb detector at the LHC, J. Instrum. **3**, S08005 (2008).
[15] R. Aaij *et al.* (LHCb Collaboration), LHCb detector performance, Int. J. Mod. Phys. A **30**, 1530022 (2015).
[16] R. Aaij *et al.* (LHCb Collaboration), The LHCb trigger and its performance in 2011, J. Instrum. **8**, P04022 (2013).
[17] T. Sjöstrand, S. Mrenna, and P. Skands, A brief introduction to PYTHIA 8.1, Comput. Phys. Commun. **178**, 852 (2008); PYTHIA 6.4 physics and manual, J. High Energy Phys. 05 (2006) 026.
[18] D. J. Lange, The EvtGen particle decay simulation package, Nucl. Instrum. Methods Phys. Res., Sect. A **462**, 152 (2001).
[19] J. Allison *et al.* (Geant4 Collaboration), GEANT4 developments and applications, IEEE Trans. Nucl. Sci. **53**, 270 (2006); S. Agostinelli *et al.* (Geant4 Collaboration), GEANT4: A simulation toolkit, Nucl. Instrum. Methods Phys. Res., Sect. A **506**, 250 (2003).
[20] V. V. Gligorov and M. Williams, Efficient, reliable and fast high-level triggering using a bonsai boosted decision tree, J. Instrum. **8**, P02013 (2013).
[21] L. Breiman, J. H. Friedman, R. A. Olshen, and C. J. Stone, *Classification and Regression Trees* (Wadsworth International Group, Belmont, CA, 1984).
[22] R. E. Schapire and Y. Freund, A decision-theoretic generalization of on-line learning and an application to boosting, J. Comput. Syst. Sci. **55**, 119 (1997).
[23] K. Abe *et al.* (SLD Collaboration), A Measurement of $R(b)$ Using a Vertex Mass Tag, Phys. Rev. Lett. **80**, 660 (1998).
[24] G. Ciezarek, A. Lupato, M. Rotondo, and M. Vesterinen, Reconstruction of semileptonically decaying beauty hadrons produced in high energy pp collisions, J. High Energy Phys. 02 (2017) 021.
[25] R. J. Barlow and C. Beeston, Fitting using finite Monte Carlo samples, Comput. Phys. Commun. **77**, 219 (1993).
[26] Particle Data Group, P. A. Zyla *et al.*, Review of particle physics, Prog. Theor. Exp. Phys. **2020**, 083C01 (2020).
[27] L. Anderlini *et al.* (LHCb Collaboration), The PIDCalib package, Report No. LHCb-PUB-2016-021, 2016.
[28] E. McLean, C. T. H. Davies, J. Koponen, and A. T. Lytle, $B_s \to D_s \ell \nu$ form factors for the full q^2 range from lattice QCD with non-perturbatively normalized currents, Phys. Rev. D **101**, 074513 (2020).
[29] C. M. Bouchard, G. Peter Lepage, C. Monahan, H. Na, and J. Shigemitsu, $B_s \to K \ell \nu$ form factors from lattice QCD, Phys. Rev. D **90**, 054506 (2014).
[30] J. M. Flynn, T. Izubuchi, T. Kawanai, C. Lehner, A. Soni, R. S. Van de Water, and O. Witzel (RBC and UKQCD Collaborations), $B \to \pi \ell \nu$ and $B_s \to K \ell \nu$ form factors and $|V_{ub}|$ from 2 + 1-flavor lattice QCD with domain-wall light quarks and relativistic heavy quarks, Phys. Rev. D **91**, 074510 (2015).
[31] A. Bazavov, C. Bernard, C. DeTar, D. Du, A. X. El-Khadra *et al.* (Fermilab Lattice and MILC Collaborations), $B_s \to K \ell \nu$ decay from lattice QCD, Phys. Rev. D **100**, 034501 (2019).
[32] A. Khodjamirian and A. V. Rusov, $B_s \to K \ell \nu_\ell$ and $B_{(s)} \to \pi(K) \ell^+ \ell^-$ decays at large recoil and CKM matrix elements, J. High Energy Phys. 08 (2017) 112.
[33] W. Detmold, C. Lehner, and S. Meinel, $\Lambda_b^0 \to p \ell^- \bar{\nu}_\ell$ and $\Lambda_b^0 \to \Lambda_c^+ \ell^- \bar{\nu}_\ell$ form factors from lattice QCD with relativistic heavy quarks, Phys. Rev. D **92**, 034503 (2015).

R. Aaij,[32] C. Abellán Beteta,[50] T. Ackernley,[60] B. Adeva,[46] M. Adinolfi,[54] H. Afsharnia,[9] C. A. Aidala,[85] S. Aiola,[26] Z. Ajaltouni,[9] S. Akar,[65] J. Albrecht,[15] F. Alessio,[48] M. Alexander,[59] A. Alfonso Albero,[45] Z. Aliouche,[62] G. Alkhazov,[38] P. Alvarez Cartelle,[48] S. Amato,[2] Y. Amhis,[11] L. An,[22] L. Anderlini,[22] A. Andreianov,[38] M. Andreotti,[21] F. Archilli,[17] A. Artamonov,[44] M. Artuso,[68] K. Arzymatov,[42] E. Aslanides,[10] M. Atzeni,[50] B. Audurier,[12] S. Bachmann,[17] M. Bachmayer,[49] J. J. Back,[56] S. Baker,[61] P. Baladron Rodriguez,[46] V. Balagura,[12] W. Baldini,[21,48] J. Baptista Leite,[1] R. J. Barlow,[62] S. Barsuk,[11] W. Barter,[61] M. Bartolini,[24,a] F. Baryshnikov,[81] J. M. Basels,[14] G. Bassi,[29] B. Batsukh,[68] A. Battig,[15] A. Bay,[49] M. Becker,[15] F. Bedeschi,[29] I. Bediaga,[1] A. Beiter,[68] V. Belavin,[42] S. Belin,[27] V. Bellee,[49] K. Belous,[44] I. Belov,[40] I. Belyaev,[39] G. Bencivenni,[23] E. Ben-Haim,[13] A. Berezhnoy,[40] R. Bernet,[50] D. Berninghoff,[17] H. C. Bernstein,[68] C. Bertella,[48] E. Bertholet,[13] A. Bertolin,[28] C. Betancourt,[50] F. Betti,[20,b] M. O. Bettler,[55] Ia. Bezshyiko,[50] S. Bhasin,[54] J. Bhom,[34] L. Bian,[73] M. S. Bieker,[15] S. Bifani,[53] P. Billoir,[13] M. Birch,[61] F. C. R. Bishop,[55] A. Bizzeti,[22,c] M. Bjørn,[63] M. P. Blago,[48] T. Blake,[56] F. Blanc,[49] S. Blusk,[68] D. Bobulska,[59] J. A. Boelhauve,[15] O. Boente Garcia,[46] T. Boettcher,[64] A. Boldyrev,[82] A. Bondar,[43] N. Bondar,[38] S. Borghi,[62] M. Borisyak,[42] M. Borsato,[17] J. T. Borsuk,[34] S. A. Bouchiba,[49] T. J. V. Bowcock,[60] A. Boyer,[48] C. Bozzi,[21] M. J. Bradley,[61] S. Braun,[66] A. Brea Rodriguez,[46] M. Brodski,[48] J. Brodzicka,[34] A. Brossa Gonzalo,[56] D. Brundu,[27] A. Buonaura,[50] C. Burr,[48] A. Bursche,[27] A. Butkevich,[41] J. S. Butter,[32] J. Buytaert,[48] W. Byczynski,[48] S. Cadeddu,[27] H. Cai,[73] R. Calabrese,[21,d] L. Calefice,[15,13] L. Calero Diaz,[23] S. Cali,[23] R. Calladine,[53] M. Calvi,[25,e] M. Calvo Gomez,[84] P. Camargo Magalhaes,[54] A. Camboni,[45] P. Campana,[23] D. H. Campora Perez,[48] A. F. Campoverde Quezada,[5] S. Capelli,[25,e] L. Capriotti,[20,b] A. Carbone,[20,b] G. Carboni,[30] R. Cardinale,[24,a] A. Cardini,[27] I. Carli,[6] P. Carniti,[25,e] L. Carus,[14] K. Carvalho Akiba,[32] A. Casais Vidal,[46] G. Casse,[60] M. Cattaneo,[48] G. Cavallero,[48] S. Celani,[49] J. Cerasoli,[10] A. J. Chadwick,[60] M. G. Chapman,[54] M. Charles,[13] Ph. Charpentier,[48] G. Chatzikonstantinidis,[53]

C. A. Chavez Barajas,[60] M. Chefdeville,[8] C. Chen,[3] S. Chen,[27] A. Chernov,[34] S.-G. Chitic,[48] V. Chobanova,[46] S. Cholak,[49] M. Chrzaszcz,[34] A. Chubykin,[38] V. Chulikov,[38] P. Ciambrone,[23] M. F. Cicala,[56] X. Cid Vidal,[46] G. Ciezarek,[48] P. E. L. Clarke,[58] M. Clemencic,[48] H. V. Cliff,[55] J. Closier,[48] J. L. Cobbledick,[62] V. Coco,[48] J. A. B. Coelho,[11] J. Cogan,[10] E. Cogneras,[9] L. Cojocariu,[37] P. Collins,[48] T. Colombo,[48] L. Congedo,[19,f] A. Contu,[27] N. Cooke,[53] G. Coombs,[59] G. Corti,[48] C. M. Costa Sobral,[56] B. Couturier,[48] D. C. Craik,[64] J. Crkovská,[67] M. Cruz Torres,[1] R. Currie,[58] C. L. Da Silva,[67] E. Dall'Occo,[15] J. Dalseno,[46] C. D'Ambrosio,[48] A. Danilina,[39] P. d'Argent,[48] A. Davis,[62] O. De Aguiar Francisco,[62] K. De Bruyn,[78] S. De Capua,[62] M. De Cian,[49] J. M. De Miranda,[1] L. De Paula,[2] M. De Serio,[19,f] D. De Simone,[50] P. De Simone,[23] J. A. de Vries,[79] C. T. Dean,[67] W. Dean,[85] D. Decamp,[8] L. Del Buono,[13] B. Delaney,[55] H.-P. Dembinski,[15] A. Dendek,[35] V. Denysenko,[50] D. Derkach,[82] O. Deschamps,[9] F. Desse,[11] F. Dettori,[27,g] B. Dey,[73] P. Di Nezza,[23] S. Didenko,[81] L. Dieste Maronas,[46] H. Dijkstra,[48] V. Dobishuk,[52] A. M. Donohoe,[18] F. Dordei,[27] A. C. dos Reis,[1] L. Douglas,[59] A. Dovbnya,[51] A. G. Downes,[8] K. Dreimanis,[60] M. W. Dudek,[34] L. Dufour,[48] V. Duk,[77] P. Durante,[48] J. M. Durham,[67] D. Dutta,[62] M. Dziewiecki,[17] A. Dziurda,[34] A. Dzyuba,[38] S. Easo,[57] U. Egede,[69] V. Egorychev,[39] S. Eidelman,[43,h] S. Eisenhardt,[58] S. Ek-In,[49] L. Eklund,[59] S. Ely,[68] A. Ene,[37] E. Epple,[67] S. Escher,[14] J. Eschle,[50] S. Esen,[32] T. Evans,[48] A. Falabella,[20] J. Fan,[3] Y. Fan,[5] B. Fang,[73] N. Farley,[53] S. Farry,[60] D. Fazzini,[25,e] P. Fedin,[39] M. Féo,[48] P. Fernandez Declara,[48] A. Fernandez Prieto,[46] J. M. Fernandez-tenllado Arribas,[45] F. Ferrari,[20,b] L. Ferreira Lopes,[49] F. Ferreira Rodrigues,[2] S. Ferreres Sole,[32] M. Ferrillo,[50] M. Ferro-Luzzi,[48] S. Filippov,[41] R. A. Fini,[19] M. Fiorini,[21,d] M. Firlej,[35] K. M. Fischer,[63] C. Fitzpatrick,[62] T. Fiutowski,[35] F. Fleuret,[12] M. Fontana,[13] F. Fontanelli,[24,a] R. Forty,[48] V. Franco Lima,[60] M. Franco Sevilla,[66] M. Frank,[48] E. Franzoso,[21] G. Frau,[17] C. Frei,[48] D. A. Friday,[59] J. Fu,[26] Q. Fuehring,[15] W. Funk,[48] E. Gabriel,[32] T. Gaintseva,[42] A. Gallas Torreira,[46] D. Galli,[20,b] S. Gambetta,[58,48] Y. Gan,[3] M. Gandelman,[2] P. Gandini,[26] Y. Gao,[4] M. Garau,[27] L. M. Garcia Martin,[56] P. Garcia Moreno,[45] J. García Pardiñas,[50] B. Garcia Plana,[46] F. A. Garcia Rosales,[12] L. Garrido,[45] C. Gaspar,[48] R. E. Geertsema,[32] D. Gerick,[17] L. L. Gerken,[15] E. Gersabeck,[62] M. Gersabeck,[62] T. Gershon,[56] D. Gerstel,[10] Ph. Ghez,[8] V. Gibson,[55] M. Giovannetti,[23,i] A. Gioventù,[46] P. Gironella Gironell,[45] L. Giubega,[37] C. Giugliano,[21,48,d] K. Gizdov,[58] E. L. Gkougkousis,[48] V. V. Gligorov,[13] C. Göbel,[70] E. Golobardes,[84] D. Golubkov,[39] A. Golutvin,[61,81] A. Gomes,[1,j] S. Gomez Fernandez,[45] F. Goncalves Abrantes,[70] M. Goncerz,[34] G. Gong,[3] P. Gorbounov,[39] I. V. Gorelov,[40] C. Gotti,[25,e] E. Govorkova,[48] J. P. Grabowski,[17] R. Graciani Diaz,[45] T. Grammatico,[13] L. A. Granado Cardoso,[48] E. Graugés,[45] E. Graverini,[49] G. Graziani,[22] A. Grecu,[37] L. M. Greeven,[32] P. Griffith,[21] L. Grillo,[62] S. Gromov,[81] B. R. Gruberg Cazon,[63] C. Gu,[3] M. Guarise,[21] P. A. Günther,[17] E. Gushchin,[41] A. Guth,[14] Y. Guz,[44,48] T. Gys,[48] T. Hadavizadeh,[69] G. Haefeli,[49] C. Haen,[48] J. Haimberger,[48] T. Halewood-leagas,[60] P. M. Hamilton,[66] Q. Han,[7] X. Han,[17] T. H. Hancock,[63] S. Hansmann-Menzemer,[17] N. Harnew,[63] T. Harrison,[60] C. Hasse,[48] M. Hatch,[48] J. He,[5] M. Hecker,[61] K. Heijhoff,[32] K. Heinicke,[15] A. M. Hennequin,[48] K. Hennessy,[60] L. Henry,[26,47] J. Heuel,[14] A. Hicheur,[2] D. Hill,[63] M. Hilton,[62] S. E. Hollitt,[15] J. Hu,[17] J. Hu,[72] W. Hu,[7] W. Huang,[5] X. Huang,[73] W. Hulsbergen,[32] R. J. Hunter,[56] M. Hushchyn,[82] D. Hutchcroft,[60] D. Hynds,[32] P. Ibis,[15] M. Idzik,[35] D. Ilin,[38] P. Ilten,[65] A. Inglessi,[38] A. Ishteev,[81] K. Ivshin,[38] R. Jacobsson,[48] S. Jakobsen,[48] E. Jans,[32] B. K. Jashal,[47] A. Jawahery,[66] V. Jevtic,[15] M. Jezabek,[34] F. Jiang,[3] M. John,[63] D. Johnson,[48] C. R. Jones,[55] T. P. Jones,[56] B. Jost,[48] N. Jurik,[48] S. Kandybei,[51] Y. Kang,[3] M. Karacson,[48] M. Karpov,[82] N. Kazeev,[82] F. Keizer,[55,48] M. Kenzie,[56] T. Ketel,[33] B. Khanji,[15] A. Kharisova,[83] S. Kholodenko,[44] K. E. Kim,[68] T. Kirn,[14] V. S. Kirsebom,[49] O. Kitouni,[64] S. Klaver,[32] K. Klimaszewski,[36] S. Koliiev,[52] A. Kondybayeva,[81] A. Konoplyannikov,[39] P. Kopciewicz,[35] R. Kopecna,[17] P. Koppenburg,[32] M. Korolev,[40] I. Kostiuk,[32,52] O. Kot,[52] S. Kotriakhova,[38,31] P. Kravchenko,[38] L. Kravchuk,[41] R. D. Krawczyk,[48] M. Kreps,[56] F. Kress,[61] S. Kretzschmar,[14] P. Krokovny,[43,h] W. Krupa,[35] W. Krzemien,[36] W. Kucewicz,[34,k] M. Kucharczyk,[34] V. Kudryavtsev,[43,h] H. S. Kuindersma,[32] G. J. Kunde,[67] T. Kvaratskheliya,[39] D. Lacarrere,[48] G. Lafferty,[62] A. Lai,[27] A. Lampis,[27] D. Lancierini,[50] J. J. Lane,[62] R. Lane,[54] G. Lanfranchi,[23] C. Langenbruch,[14] J. Langer,[15] O. Lantwin,[50,81] T. Latham,[56] F. Lazzari,[29,l] R. Le Gac,[10] S. H. Lee,[85] R. Lefèvre,[9] A. Leflat,[40] S. Legotin,[81] O. Leroy,[10] T. Lesiak,[34] B. Leverington,[17] H. Li,[72] L. Li,[63] P. Li,[17] Y. Li,[6] Y. Li,[6] Z. Li,[68] X. Liang,[68] T. Lin,[61] R. Lindner,[48] V. Lisovskyi,[15] R. Litvinov,[27] G. Liu,[72] H. Liu,[5] S. Liu,[6] X. Liu,[3] A. Loi,[27] J. Lomba Castro,[46] I. Longstaff,[59] J. H. Lopes,[2] G. Loustau,[50] G. H. Lovell,[55] Y. Lu,[6] D. Lucchesi,[28,m] S. Luchuk,[41] M. Lucio Martinez,[32] V. Lukashenko,[32] Y. Luo,[3] A. Lupato,[62] E. Luppi,[21,d] O. Lupton,[56] A. Lusiani,[29,n] X. Lyu,[5] L. Ma,[6] S. Maccolini,[20,b] F. Machefert,[11] F. Maciuc,[37] V. Macko,[49] P. Mackowiak,[15] S. Maddrell-Mander,[54] O. Madejczyk,[35] L. R. Madhan Mohan,[54] O. Maev,[38] A. Maevskiy,[82] D. Maisuzenko,[38] M. W. Majewski,[35] J. J. Malczewski,[34] S. Malde,[63] B. Malecki,[48] A. Malinin,[80] T. Maltsev,[43,h] H. Malygina,[17] G. Manca,[27,g] G. Mancinelli,[10] R. Manera Escalero,[45] D. Manuzzi,[20,b] D. Marangotto,[26,o] J. Maratas,[9,p] J. F. Marchand,[8] U. Marconi,[20] S. Mariani,[22,48,q] C. Marin Benito,[11]

M. Marinangeli,[49] P. Marino,[49] J. Marks,[17] P. J. Marshall,[60] G. Martellotti,[31] L. Martinazzoli,[48,e] M. Martinelli,[25,e] D. Martinez Santos,[46] F. Martinez Vidal,[47] A. Massafferri,[1] M. Materok,[14] R. Matev,[48] A. Mathad,[50] Z. Mathe,[48] V. Matiunin,[39] C. Matteuzzi,[25] K. R. Mattioli,[85] A. Mauri,[32] E. Maurice,[12] J. Mauricio,[45] M. Mazurek,[36] M. McCann,[61] L. Mcconnell,[18] T. H. Mcgrath,[62] A. McNab,[62] R. McNulty,[18] J. V. Mead,[60] B. Meadows,[65] C. Meaux,[10] G. Meier,[15] N. Meinert,[76] D. Melnychuk,[36] S. Meloni,[25,e] M. Merk,[32,79] A. Merli,[26] L. Meyer Garcia,[2] M. Mikhasenko,[48] D. A. Milanes,[74] E. Millard,[56] M. Milovanovic,[48] M.-N. Minard,[8] L. Minzoni,[21,d] S. E. Mitchell,[58] B. Mitreska,[62] D. S. Mitzel,[48] A. Mödden,[15] R. A. Mohammed,[63] R. D. Moise,[61] T. Mombächer,[15] I. A. Monroy,[74] S. Monteil,[9] M. Morandin,[28] G. Morello,[23] M. J. Morello,[29,n] J. Moron,[35] A. B. Morris,[75] A. G. Morris,[56] R. Mountain,[68] H. Mu,[3] F. Muheim,[58] M. Mukherjee,[7] M. Mulder,[48] D. Müller,[48] K. Müller,[50] C. H. Murphy,[63] D. Murray,[62] P. Muzzetto,[27,48] P. Naik,[54] T. Nakada,[49] R. Nandakumar,[57] T. Nanut,[49] I. Nasteva,[2] M. Needham,[58] I. Neri,[21,d] N. Neri,[26,o] S. Neubert,[75] N. Neufeld,[48] R. Newcombe,[61] T. D. Nguyen,[49] C. Nguyen-Mau,[49] E. M. Niel,[11] S. Nieswand,[14] N. Nikitin,[40] N. S. Nolte,[48] C. Nunez,[85] A. Oblakowska-Mucha,[35] V. Obraztsov,[44] D. P. O'Hanlon,[54] R. Oldeman,[27,g] M. E. Olivares,[68] C. J. G. Onderwater,[78] A. Ossowska,[34] J. M. Otalora Goicochea,[2] T. Ovsiannikova,[39] P. Owen,[50] A. Oyanguren,[47,48] B. Pagare,[56] P. R. Pais,[48] T. Pajero,[29,48,n] A. Palano,[19] M. Palutan,[23] Y. Pan,[62] G. Panshin,[83] A. Papanestis,[57] M. Pappagallo,[19,f] L. L. Pappalardo,[21,d] C. Pappenheimer,[65] W. Parker,[66] C. Parkes,[62] C. J. Parkinson,[46] B. Passalacqua,[21] G. Passaleva,[22] A. Pastore,[19] M. Patel,[61] C. Patrignani,[20,b] C. J. Pawley,[79] A. Pearce,[48] A. Pellegrino,[32] M. Pepe Altarelli,[48] S. Perazzini,[20] D. Pereima,[39] P. Perret,[9] K. Petridis,[54] A. Petrolini,[24,a] A. Petrov,[80] S. Petrucci,[58] M. Petruzzo,[26] T. T. H. Pham,[68] A. Philippov,[42] L. Pica,[29] M. Piccini,[77] B. Pietrzyk,[8] G. Pietrzyk,[49] M. Pili,[63] D. Pinci,[31] F. Pisani,[48] A. Piucci,[17] Resmi P. K,[10] V. Placinta,[37] J. Plews,[53] M. Plo Casasus,[46] F. Polci,[13] M. Poli Lener,[23] M. Poliakova,[68] A. Poluektov,[10] N. Polukhina,[81,r] I. Polyakov,[68] E. Polycarpo,[2] G. J. Pomery,[54] S. Ponce,[48] D. Popov,[5,48] S. Popov,[42] S. Poslavskii,[44] K. Prasanth,[34] L. Promberger,[48] C. Prouve,[46] V. Pugatch,[52] H. Pullen,[63] G. Punzi,[29,s] W. Qian,[5] J. Qin,[5] R. Quagliani,[13] B. Quintana,[8] N. V. Raab,[18] R. I. Rabadan Trejo,[10] B. Rachwal,[35] J. H. Rademacker,[54] M. Rama,[29] M. Ramos Pernas,[56] M. S. Rangel,[2] F. Ratnikov,[42,82] G. Raven,[33] M. Reboud,[8] F. Redi,[49] F. Reiss,[13] C. Remon Alepuz,[47] Z. Ren,[3] V. Renaudin,[63] R. Ribatti,[29] S. Ricciardi,[57] K. Rinnert,[60] P. Robbe,[11] A. Robert,[13] G. Robertson,[58] A. B. Rodrigues,[49] E. Rodrigues,[60] J. A. Rodriguez Lopez,[74] A. Rollings,[63] P. Roloff,[48] V. Romanovskiy,[44] M. Romero Lamas,[46] A. Romero Vidal,[46] J. D. Roth,[85] M. Rotondo,[23] M. S. Rudolph,[68] T. Ruf,[48] J. Ruiz Vidal,[47] A. Ryzhikov,[82] J. Ryzka,[35] J. J. Saborido Silva,[46] N. Sagidova,[38] N. Sahoo,[56] B. Saitta,[27,g] D. Sanchez Gonzalo,[45] C. Sanchez Gras,[32] R. Santacesaria,[31] C. Santamarina Rios,[46] M. Santimaria,[23] E. Santovetti,[30,i] D. Saranin,[81] G. Sarpis,[59] M. Sarpis,[75] A. Sarti,[31] C. Satriano,[31,t] A. Satta,[30] M. Saur,[5] D. Savrina,[39,40] H. Sazak,[9] L. G. Scantlebury Smead,[63] S. Schael,[14] M. Schellenberg,[15] M. Schiller,[59] H. Schindler,[48] M. Schmelling,[16] T. Schmelzer,[15] B. Schmidt,[48] O. Schneider,[49] A. Schopper,[48] M. Schubiger,[32] S. Schulte,[49] M. H. Schune,[11] R. Schwemmer,[48] B. Sciascia,[23] A. Sciubba,[31] S. Sellam,[46] A. Semennikov,[39] M. Senghi Soares,[33] A. Sergi,[53,48] N. Serra,[50] L. Sestini,[28] A. Seuthe,[15] P. Seyfert,[48] D. M. Shangase,[85] M. Shapkin,[44] I. Shchemerov,[81] L. Shchutska,[49] T. Shears,[60] L. Shekhtman,[43,h] Z. Shen,[4] V. Shevchenko,[80] E. B. Shields,[25,e] E. Shmanin,[81] J. D. Shupperd,[68] B. G. Siddi,[21] R. Silva Coutinho,[50] G. Simi,[28] S. Simone,[19,f] I. Skiba,[21,d] N. Skidmore,[75] T. Skwarnicki,[68] M. W. Slater,[53] J. C. Smallwood,[63] J. G. Smeaton,[55] A. Smetkina,[39] E. Smith,[14] I. T. Smith,[57] M. Smith,[61] A. Snoch,[32] M. Soares,[20] L. Soares Lavra,[9] M. D. Sokoloff,[65] F. J. P. Soler,[59] A. Solovev,[38] I. Solovyev,[38] F. L. Souza De Almeida,[2] B. Souza De Paula,[2] B. Spaan,[15] E. Spadaro Norella,[26,o] P. Spradlin,[59] F. Stagni,[48] M. Stahl,[65] S. Stahl,[48] P. Stefko,[49] O. Steinkamp,[50,81] S. Stemmle,[17] O. Stenyakin,[44] H. Stevens,[15] S. Stone,[68] M. E. Stramaglia,[49] M. Straticiuc,[37] D. Strekalina,[81] S. Strokov,[83] F. Suljik,[63] J. Sun,[27] L. Sun,[73] Y. Sun,[66] P. Svihra,[62] P. N. Swallow,[53] K. Swientek,[35] A. Szabelski,[36] T. Szumlak,[35] M. Szymanski,[48] S. Taneja,[62] F. Teubert,[48] E. Thomas,[48] K. A. Thomson,[60] M. J. Tilley,[61] V. Tisserand,[9] S. T'Jampens,[8] M. Tobin,[6] S. Tolk,[48] L. Tomassetti,[21,d] D. Torres Machado,[1] D. Y. Tou,[13] M. Traill,[59] M. T. Tran,[49] E. Trifonova,[81] C. Trippl,[49] G. Tuci,[29,s] A. Tully,[49] N. Tuning,[32] A. Ukleja,[36] D. J. Unverzagt,[17] E. Ursov,[81] A. Usachov,[32] A. Ustyuzhanin,[42,82] U. Uwer,[17] A. Vagner,[83] V. Vagnoni,[20] A. Valassi,[48] G. Valenti,[20] N. Valls Canudas,[45] M. van Beuzekom,[32] M. Van Dijk,[49] E. van Herwijnen,[81] C. B. Van Hulse,[18] M. van Veghel,[78] R. Vazquez Gomez,[46] P. Vazquez Regueiro,[46] C. Vázquez Sierra,[32] S. Vecchi,[21] J. J. Velthuis,[54] M. Veltri,[22,u] A. Venkateswaran,[68] M. Veronesi,[32] M. Vesterinen,[56] D. Vieira,[65] M. Vieites Diaz,[49] H. Viemann,[76] X. Vilasis-Cardona,[84] E. Vilella Figueras,[60] P. Vincent,[13] G. Vitali,[29] A. Vollhardt,[50] D. Vom Bruch,[13] A. Vorobyev,[38] V. Vorobyev,[43,h] N. Voropaev,[38] R. Waldi,[76] J. Walsh,[29] C. Wang,[17] J. Wang,[3] J. Wang,[73] J. Wang,[4] J. Wang,[6] M. Wang,[3] R. Wang,[54] Y. Wang,[7] Z. Wang,[50] H. M. Wark,[60] N. K. Watson,[53] S. G. Weber,[13]

D. Websdale,[61] C. Weisser,[64] B. D. C. Westhenry,[54] D. J. White,[62] M. Whitehead,[54] D. Wiedner,[15] G. Wilkinson,[63] M. Wilkinson,[68] I. Williams,[55] M. Williams,[64,69] M. R. J. Williams,[58] F. F. Wilson,[57] W. Wislicki,[36] M. Witek,[34] L. Witola,[17] G. Wormser,[11] S. A. Wotton,[55] H. Wu,[68] K. Wyllie,[48] Z. Xiang,[5] D. Xiao,[7] Y. Xie,[7] A. Xu,[4] J. Xu,[5] L. Xu,[3] M. Xu,[7] Q. Xu,[5] Z. Xu,[5] Z. Xu,[4] D. Yang,[3] Y. Yang,[5] Z. Yang,[3] Z. Yang,[66] Y. Yao,[68] L. E. Yeomans,[60] H. Yin,[7] J. Yu,[71] X. Yuan,[68] O. Yushchenko,[44] E. Zaffaroni,[49] K. A. Zarebski,[53] M. Zavertyaev,[16,r] M. Zdybal,[34] O. Zenaiev,[48] M. Zeng,[3] D. Zhang,[7] L. Zhang,[3] S. Zhang,[4] Y. Zhang,[4] Y. Zhang,[63] A. Zhelezov,[17] Y. Zheng,[5] X. Zhou,[5] Y. Zhou,[5] X. Zhu,[3] V. Zhukov,[14,40] J. B. Zonneveld,[58] S. Zucchelli,[20,b] D. Zuliani,[28] and G. Zunica[62]

(LHCb Collaboration)

[1]*Centro Brasileiro de Pesquisas Físicas (CBPF), Rio de Janeiro, Brazil*
[2]*Universidade Federal do Rio de Janeiro (UFRJ), Rio de Janeiro, Brazil*
[3]*Center for High Energy Physics, Tsinghua University, Beijing, China*
[4]*School of Physics State Key Laboratory of Nuclear Physics and Technology, Peking University, Beijing, China*
[5]*University of Chinese Academy of Sciences, Beijing, China*
[6]*Institute Of High Energy Physics (IHEP), Beijing, China*
[7]*Institute of Particle Physics, Central China Normal University, Wuhan, Hubei, China*
[8]*Univ. Grenoble Alpes, Univ. Savoie Mont Blanc, CNRS, IN2P3-LAPP, Annecy, France*
[9]*Université Clermont Auvergne, CNRS/IN2P3, LPC, Clermont-Ferrand, France*
[10]*Aix Marseille Univ, CNRS/IN2P3, CPPM, Marseille, France*
[11]*Université Paris-Saclay, CNRS/IN2P3, IJCLab, Orsay, France*
[12]*Laboratoire Leprince-ringuet (llr), Palaiseau, France*
[13]*LPNHE, Sorbonne Université, Paris Diderot Sorbonne Paris Cité, CNRS/IN2P3, Paris, France*
[14]*I. Physikalisches Institut, RWTH Aachen University, Aachen, Germany*
[15]*Fakultät Physik, Technische Universität Dortmund, Dortmund, Germany*
[16]*Max-Planck-Institut für Kernphysik (MPIK), Heidelberg, Germany*
[17]*Physikalisches Institut, Ruprecht-Karls-Universität Heidelberg, Heidelberg, Germany*
[18]*School of Physics, University College Dublin, Dublin, Ireland*
[19]*INFN Sezione di Bari, Bari, Italy*
[20]*INFN Sezione di Bologna, Bologna, Italy*
[21]*INFN Sezione di Ferrara, Ferrara, Italy*
[22]*INFN Sezione di Firenze, Firenze, Italy*
[23]*INFN Laboratori Nazionali di Frascati, Frascati, Italy*
[24]*INFN Sezione di Genova, Genova, Italy*
[25]*INFN Sezione di Milano-Bicocca, Milano, Italy*
[26]*INFN Sezione di Milano, Milano, Italy*
[27]*INFN Sezione di Cagliari, Monserrato, Italy*
[28]*Universita degli Studi di Padova, Universita e INFN, Padova, Padova, Italy*
[29]*INFN Sezione di Pisa, Pisa, Italy*
[30]*INFN Sezione di Roma Tor Vergata, Roma, Italy*
[31]*INFN Sezione di Roma La Sapienza, Roma, Italy*
[32]*Nikhef National Institute for Subatomic Physics, Amsterdam, Netherlands*
[33]*Nikhef National Institute for Subatomic Physics and VU University Amsterdam, Amsterdam, Netherlands*
[34]*Henryk Niewodniczanski Institute of Nuclear Physics Polish Academy of Sciences, Kraków, Poland*
[35]*AGH—University of Science and Technology, Faculty of Physics and Applied Computer Science, Kraków, Poland*
[36]*National Center for Nuclear Research (NCBJ), Warsaw, Poland*
[37]*Horia Hulubei National Institute of Physics and Nuclear Engineering, Bucharest-Magurele, Romania*
[38]*Petersburg Nuclear Physics Institute NRC Kurchatov Institute (PNPI NRC KI), Gatchina, Russia*
[39]*Institute of Theoretical and Experimental Physics NRC Kurchatov Institute (ITEP NRC KI), Moscow, Russia*
[40]*Institute of Nuclear Physics, Moscow State University (SINP MSU), Moscow, Russia*
[41]*Institute for Nuclear Research of the Russian Academy of Sciences (INR RAS), Moscow, Russia*
[42]*Yandex School of Data Analysis, Moscow, Russia*
[43]*Budker Institute of Nuclear Physics (SB RAS), Novosibirsk, Russia*
[44]*Institute for High Energy Physics NRC Kurchatov Institute (IHEP NRC KI), Protvino, Russia, Protvino, Russia*
[45]*ICCUB, Universitat de Barcelona, Barcelona, Spain*
[46]*Instituto Galego de Física de Altas Enerxías (IGFAE), Universidade de Santiago de Compostela, Santiago de Compostela, Spain*
[47]*Instituto de Fisica Corpuscular, Centro Mixto Universidad de Valencia—CSIC, Valencia, Spain*

[48]European Organization for Nuclear Research (CERN), Geneva, Switzerland
[49]Institute of Physics, Ecole Polytechnique Fédérale de Lausanne (EPFL), Lausanne, Switzerland
[50]Physik-Institut, Universität Zürich, Zürich, Switzerland
[51]NSC Kharkiv Institute of Physics and Technology (NSC KIPT), Kharkiv, Ukraine
[52]Institute for Nuclear Research of the National Academy of Sciences (KINR), Kyiv, Ukraine
[53]University of Birmingham, Birmingham, United Kingdom
[54]H.H. Wills Physics Laboratory, University of Bristol, Bristol, United Kingdom
[55]Cavendish Laboratory, University of Cambridge, Cambridge, United Kingdom
[56]Department of Physics, University of Warwick, Coventry, United Kingdom
[57]STFC Rutherford Appleton Laboratory, Didcot, United Kingdom
[58]School of Physics and Astronomy, University of Edinburgh, Edinburgh, United Kingdom
[59]School of Physics and Astronomy, University of Glasgow, Glasgow, United Kingdom
[60]Oliver Lodge Laboratory, University of Liverpool, Liverpool, United Kingdom
[61]Imperial College London, London, United Kingdom
[62]Department of Physics and Astronomy, University of Manchester, Manchester, United Kingdom
[63]Department of Physics, University of Oxford, Oxford, United Kingdom
[64]Massachusetts Institute of Technology, Cambridge, Massachusetts, USA
[65]University of Cincinnati, Cincinnati, Ohio, USA
[66]University of Maryland, College Park, Maryland, USA
[67]Los Alamos National Laboratory (LANL), Los Alamos, United States
[68]Syracuse University, Syracuse, New York, USA
[69]School of Physics and Astronomy, Monash University, Melbourne, Australia
(associated with Department of Physics, University of Warwick, Coventry, United Kingdom)
[70]Pontifícia Universidade Católica do Rio de Janeiro (PUC-Rio), Rio de Janeiro, Brazil
[associated with Universidade Federal do Rio de Janeiro (UFRJ), Rio de Janeiro, Brazil]
[71]Physics and Micro Electronic College, Hunan University, Changsha City, China
(associated with Institute of Particle Physics, Central China Normal University, Wuhan, Hubei, China)
[72]Guangdong Provencial Key Laboratory of Nuclear Science, Institute of Quantum Matter, South China Normal University, Guangzhou, China
(associated with Center for High Energy Physics, Tsinghua University, Beijing, China)
[73]School of Physics and Technology, Wuhan University, Wuhan, China
(associated with Center for High Energy Physics, Tsinghua University, Beijing, China)
[74]Departamento de Fisica, Universidad Nacional de Colombia, Bogota, Colombia
(associated with LPNHE, Sorbonne Université, Paris Diderot Sorbonne Paris Cite, CNRS/IN2P3, Paris, France)
[75]Universität Bonn—Helmholtz-Institut für Strahlen und Kernphysik, Bonn, Germany
(associated with Physikalisches Institut, Ruprecht-Karls-Universitat Heidelberg, Heidelberg, Germany)
[76]Institut für Physik, Universität Rostock, Rostock, Germany
(associated with Physikalisches Institut, Ruprecht-Karls-Universitat Heidelberg, Heidelberg, Germany)
[77]INFN Sezione di Perugia, Perugia, Italy (associated with INFN Sezione di Ferrara, Ferrara, Italy)
[78]Van Swinderen Institute, University of Groningen, Groningen, Netherlands
(associated with Nikhef National Institute for Subatomic Physics, Amsterdam, Netherlands)
[79]Universiteit Maastricht, Maastricht, Netherlands
(associated with Nikhef National Institute for Subatomic Physics, Amsterdam, Netherlands)
[80]National Research Centre Kurchatov Institute, Moscow, Russia
[associated with Institute of Theoretical and Experimental Physics NRC Kurchatov Institute (ITEP NRC KI), Moscow, Russia]
[81]National University of Science and Technology "MISIS", Moscow, Russia
[associated with Institute of Theoretical and Experimental Physics NRC Kurchatov Institute (ITEP NRC KI), Moscow, Russia]
[82]National Research University Higher School of Economics, Moscow, Russia
(associated with Yandex School of Data Analysis, Moscow, Russia)
[83]National Research Tomsk Polytechnic University, Tomsk, Russia
[associated with Institute of Theoretical and Experimental Physics NRC Kurchatov Institute (ITEP NRC KI), Moscow, Russia]
[84]DS4DS, La Salle, Universitat Ramon Llull, Barcelona, Spain
(associated with ICCUB, Universitat de Barcelona, Barcelona, Spain)
[85]University of Michigan, Ann Arbor, Michigan, USA
(associated with Syracuse University, Syracuse, New York, USA)

[a]Also at Università di Genova, Genova, Italy.
[b]Also at Università di Bologna, Bologna, Italy.
[c]Also at Università di Modena e Reggio Emilia, Modena, Italy.
[d]Also at Università di Ferrara, Ferrara, Italy.

[e]Also at Università di Milano Bicocca, Milano, Italy.
[f]Also at Università di Bari, Bari, Italy.
[g]Also at Università di Cagliari, Cagliari, Italy.
[h]Also at Novosibirsk State University, Novosibirsk, Russia.
[i]Also at Università di Roma Tor Vergata, Roma, Italy.
[j]Also at Universidade Federal do Triângulo Mineiro (UFTM), Uberaba-MG, Brazil.
[k]Also at AGH—University of Science and Technology, Faculty of Computer Science, Electronics and Telecommunications, Kraków, Poland.
[l]Also at Università di Siena, Siena, Italy.
[m]Also at Università di Padova, Padova, Italy.
[n]Also at Scuola Normale Superiore, Pisa, Italy.
[o]Also at Università degli Studi di Milano, Milano, Italy.
[p]Also at MSU—Iligan Institute of Technology (MSU-IIT), Iligan, Philippines.
[q]Also at Università di Firenze, Firenze, Italy.
[r]Also at P.N. Lebedev Physical Institute, Russian Academy of Science (LPI RAS), Moscow, Russia.
[s]Also at Università di Pisa, Pisa, Italy.
[t]Also at Università della Basilicata, Potenza, Italy.
[u]Also at Università di Urbino, Urbino, Italy.